

Diffusion of Gold from the Inner Core to the Surface of Ag₂S Nanocrystals

Jun Yang and Jackie Y. Ying*

Institute of Bioengineering and Nanotechnology, 31 Biopolis Way, The Nanos, Singapore 138669

Received October 25, 2009; E-mail: jyying@ibn.a-star.edu.sg

The diffusion of metals in semiconductors has been extensively investigated in bulk materials due to its technological importance for applications in doped materials, catalysts, and functional spintronic devices.¹ In contrast, relatively little has been reported on diffusion in nanostructured materials, which exhibit physical and chemical properties distinctively different from bulk materials.² Recently, Banin and co-workers reported the diffusion of Au in InAs nanoparticles at room temperature, which resulted in a Au core coated by an amorphous InAs shell.^{3a} Manna et al. also described the diffusion of Au in PbTe nanocrystals at elevated temperature.^{3b} Herein, we present the diffusion of Au in Ag₂S nanocrystals from the core to the surface, giving rise to Ag₂S–Au heterodimers. This reverse diffusion of Au not only has scientific significance but also could be used to synthesize complex semiconductor–metal nanocomposites, which might not be obtainable by direct synthesis. Specifically, we demonstrated the synthesis of heterogeneous nanocomposites of core–shell Pt@Ag₂S and Au nanoparticles based on the diffusion of Au in Ag₂S nanocrystals. Ostwald ripening was observed during the characterization of the nanocomposites with transmission electron microscopy (TEM). This elucidated the mechanism of formation of semiconductor–metal heterostructures as a consequence of Au diffusion in Ag₂S nanocrystals.

The synthesis of core–shell Au@Ag₂S nanoparticles followed the seed-mediated growth method.⁴ TEM and high-angle scanning transmission electron microscopy (STEM) images are shown in Figure 1a,c, respectively, whereby the core and shell components can be easily differentiated by brightness contrast. The diffusion of Au in Ag₂S from core to surface was completed after 72 h of aging (Figures 1b,d). The resulting Ag₂S–Au heterodimers were clearly distinct from the starting core–shell Au@Ag₂S nanoparticles. Energy-dispersive X-ray (EDX) analyses (Figure 1e,f) of an arbitrary single particle before and after 72 h of aging under the STEM mode showed that gold moved from the core of the Au@Ag₂S nanoparticle to the surface of the Ag₂S nanocrystal, forming a Ag₂S–Au heterodimer. The high-resolution TEM (HR-TEM) images and X-ray diffraction (XRD) patterns (Figure S2, Supporting Information) of the starting core–shell Au@Ag₂S nanoparticles and the resulting Ag₂S–Au heterodimers confirmed that Ag₂S remained crystalline after the diffusion of Au from the core to the surface. This was quite different from the InAs–Au and PbTe–Au systems, whereby an amorphous shell of InAs and PbTe, respectively, was left behind after the diffusion of Au from the surface to the core.³

The Au seeds, core–shell Au@Ag₂S nanoparticles, and resulting Ag₂S–Au heterodimers were analyzed by X-ray photoelectron spectroscopy (XPS) (Figure S3a, Supporting Information). In comparison with the Au 4f_{7/2} and 4f_{5/2} binding energies of pure Au seeds (84.2 and 87.9 eV, respectively), an appreciable shift to higher values was observed in the core–shell Au@Ag₂S nanoparticles (84.7 and 88.4 eV, respectively) and Ag₂S–Au heterodimers (84.5 and 88.2 eV, respectively), suggesting that electrons were transferred

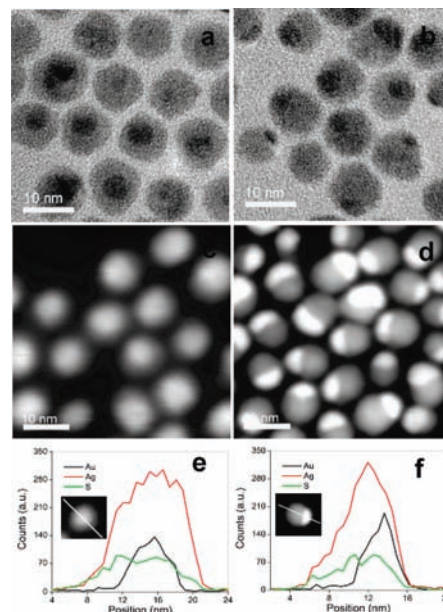


Figure 1. Diffusion of Au from the inner core to the surface of core–shell Au@Ag₂S nanoparticles: (a, b) TEM images, (c, d) STEM images, and (e, f) elemental profiles of the core–shell Au@Ag₂S nanoparticle(s) (a, c, e) as prepared and (b, d, f) after 72 h of aging.

from Au to Ag₂S. This electron-donating effect from Au to Ag₂S could be explained by intraparticle charge transfer (see Figure S3b in the Supporting Information for the energy level diagram). Comparison of the work function of Au (−5.10 eV)⁵ and the electron affinity of bulk Ag₂S (−5.32 eV)⁶ predicts that the alignment of energy levels in Au and Ag₂S would be favorable for electron transfer from Au to Ag₂S. Thus, the diffusion of Au in Ag₂S could be interpreted by the substitutional-interstitial mechanism, which occurs in numerous systems, including the diffusion of elements in silicon and germanium.⁷ As illustrated in Figure 2, after the electron transfer from Au to Ag₂S, Au ion substitutes for Ag ion in the Ag₂S lattice and diffuses for some distance before moving to the next substitutional site. Eventually, Au ions diffuse to the surface of Ag₂S and capture the electrons, which undergo interstitial diffusion in Ag₂S lattices, forming patches on the surface. This diffusion process could be achieved so that the entire system was decreased in chemical potential and reduced in Gibbs free energy.

This diffusion phenomenon could be adopted to synthesize more complex semiconductor–metal nanocomposites (see Figure 3a). Core–shell Pt@Au nanoparticles were first prepared using the seed-mediated growth method (Figure S5, Supporting Information) and then coated with Ag₂S. Au then diffused to the surface of Ag₂S, resulting in a heterogeneous hybrid of core–shell Pt@Ag₂S and Au nanoparticles (labeled as Pt@Ag₂S–Au). It should be noted that core–shell Pt@Ag₂S nanoparticles could not be synthesized

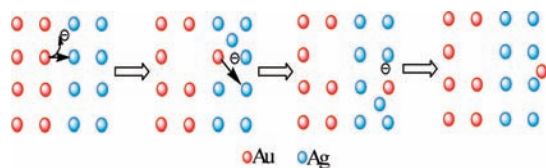


Figure 2. Schematic of Au diffusion in Ag_2S from the core to the surface via a substitutional-interstitial mechanism.

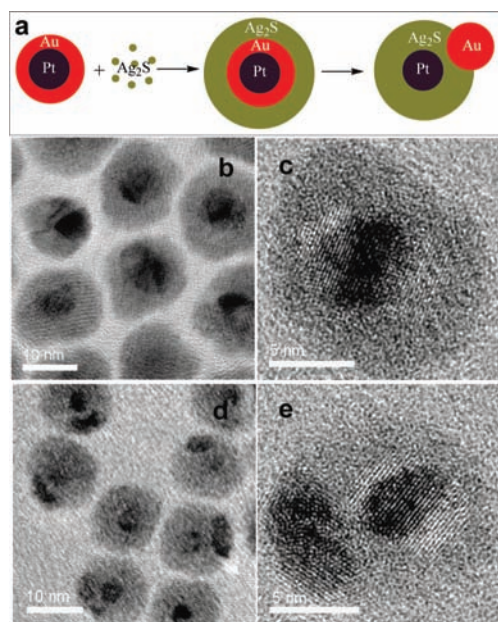


Figure 3. (a) Schematic of the synthesis of a complex semiconductor-metal nanocomposite based on the diffusion of Au in Ag_2S . (b) TEM and (c) HRTEM images of core-shell-shell $\text{Pt@Au@Ag}_2\text{S}$ nanoparticles. (d) TEM and (e) HRTEM images of the resulting $\text{Pt@Ag}_2\text{S-Au}$ nanocomposites obtained via the diffusion of Au to the surface of Ag_2S .

directly; Ag_2S nanocrystals would be formed independently as separate particles in solution in the presence of Pt seeds (Figure S7, Supporting Information).

TEM and HRTEM images of core-shell-shell $\text{Pt@Au@Ag}_2\text{S}$ nanoparticles are shown in Figure 3b,c, respectively. After 24 h of aging, Au was separated from the Pt core and diffused to the surface of Ag_2S , resulting in the formation of $\text{Pt@Ag}_2\text{S-Au}$ nanocomposites. The brightness contrast in the TEM image (Figure 3d) showed three different domains in each $\text{Pt@Ag}_2\text{S-Au}$ nanocomposite particle. The HRTEM image (Figure 3e) further revealed that the lattice orientation of the dark patch on the surface of a nanocomposite particle was different from that of the core. An EDX analyzer attached to the FEI Tecnai G² F20 TEM operating in the STEM mode was used to analyze the components in different regions of the $\text{Pt@Ag}_2\text{S-Au}$ system. The electron beam was only 0.7 nm in diameter, capable of providing a high-resolution analysis. STEM studies (Figure S6, Supporting Information) showed the confinement of each component to different regions, confirming the “patch” on the particle surface to be Au and the core of the particle to be Pt. Two sets of consistent data were obtained, demonstrating the reliability and reproducibility of the EDX analysis.

Ostwald ripening was observed during the characterization of the heterostructured nanocomposites. Ostwald ripening is a phenomenon whereby particles larger than a critical size grow at the expense of smaller particles due to their relative stabilization by

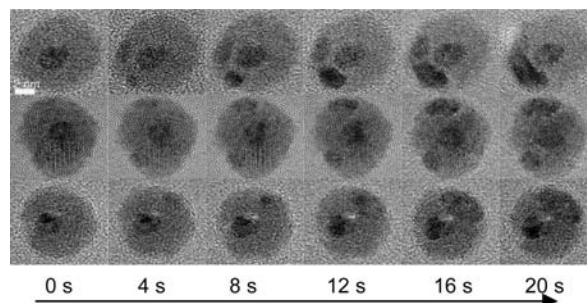


Figure 4. Ostwald ripening observed during the diffusion of Au in Ag_2S . Initially, Au diffused homogeneously in Ag_2S but then evolved as growing nanocrystals on the Ag_2S surface due to Ostwald ripening.

the surface energy term.⁸ Figure 4 shows the TEM images of three nanocomposite particles captured over a period of 20 s. Evolution of Au “patches” on the surface of the nanocomposites was clearly illustrated. The ripening observed in TEM might not exactly represent the case in solution, since the electron beam might have affected the process. However, this observation suggested why the diffusion process did not lead to a homogeneous distribution of Au on the particle surface. Initially, Au atoms might have diffused in all directions within Ag_2S . However, nanocrystals of Au were then formed on the Ag_2S surface and grew steadily due to Ostwald ripening.

In summary, the diffusion of Au in Ag_2S from the core to the surface is reported. In the first stage, Au atoms diffuse uniformly in Ag_2S from the core to the surface of Ag_2S . Au nanocrystals then evolve on the surface of Ag_2S due to Ostwald ripening. As an application of this diffusion phenomenon, a nanocomposite of core-shell $\text{Pt@Ag}_2\text{S}$ and Au nanoparticles has been synthesized for the first time. This diffusion process provides a new strategy for the synthesis of semiconductor-metal hybrids and for the metal doping in semiconductor nanocrystals.

Acknowledgment. This work was funded by the Institute of Bioengineering and Nanotechnology (Biomedical Research Council, Agency for Science, Technology and Research, Singapore).

Supporting Information Available: Text and figures giving experimental protocols, TEM images of Au seeds, Pt seeds, core-shell Pt@Au nanoparticles, and Ag_2S nanocrystals synthesized in the presence of Pt seeds, HRTEM images, XRD patterns and Au 4f XPS spectra of the core-shell $\text{Au@Ag}_2\text{S}$ nanoparticles and $\text{Ag}_2\text{S-Au}$ heterodimers, and STEM analyses of Pt@Au nanoparticles and $\text{Pt@Ag}_2\text{S-Au}$ nanocomposites. This material is available free of charge via the Internet at <http://pubs.acs.org>.

References

- (1) (a) Svoboda, J.; Fischer, F. D.; Fratzl, P.; Kroupa, A. *Acta Mater.* **2002**, *50*, 1369. (b) Matsukawa, K.; Shirai, K.; Yamaguchi, H.; Katayama-Yoshida, H. *Phys. B* **2007**, *401–402*, 151. (c) Höglund, A.; Castleton, C. W. M.; Mirbt, S. *Phys. Rev. B* **2008**, *77*, 113201. (d) Baykov, V. I.; Korzhavyi, P. A.; Johansson, B. *Phys. Rev. Lett.* **2008**, *101*, 177204. (e) Yu, H.-C.; Ven, A. V.; Thornton, K. *Phys. Rev. Lett.* **2008**, *93*, 091908.
- (2) (a) Schmid, G. *Chem. Rev.* **1992**, *92*, 1709. (b) Alivisatos, A. P. *J. Phys. Chem.* **1996**, *100*, 13226. (c) Nie, S.; Emory, S. R. *Science* **1997**, *275*, 1102.
- (3) (a) Mokari, T.; Aharoni, A.; Popov, I.; Banin, U. *Angew. Chem., Int. Ed.* **2006**, *45*, 8001. (b) Franchini, I. R.; Bertoni, G.; Falqui, A.; Giannini, C.; Wang, L. W.; Manna, L. *J. Mater. Chem.* **2010**, DOI: 1039/b915687a.
- (4) Yang, J.; Ying, J. Y. *Chem. Commun.* **2009**, 3187.
- (5) Eastman, D. E. *Phys. Rev. B* **1970**, *2*, 1.
- (6) Pelizzetti, E.; Schiavello, M., Eds. *Photochemical Conversion and Storage of Solar Energy*; Springer: New York, 1990; p 380.
- (7) Tzeli, D.; Petsalakis, I. D.; Theodorakopoulos, G. *J. Phys. Chem. C* **2009**, *113*, 13924.
- (8) Ostwald, W. F. *Z. Phys. Chem.* **1897**, *22*, 289.

JA909078P